Research Article

Apoptotic Responses Mediated by Nostoc-Synthesized Silver Nanoparticles against Ehrlich Ascites Carcinoma Tumor-Bearing Mice

Reham Samir Hamida ,[1] Gadah Albasher,[2] and Mashael Mohammed Bin-Meferij [3,4]

[1]*Molecular Biology Unit, Department of Zoology, Faculty of Science, Alexandria University, Alexandria, Egypt*
[2]*Zoology Department, College of Science, King Saud University, Riyadh, Saudi Arabia*
[3]*Department of Biology, College of Science, Princess Nourah bint Abdulrahman University, Riyadh, Saudi Arabia*
[4]*Histopathology Unit, Research Department, Health Sciences Research Center (HSRC),*
Princess Nourah bint Abdulrahman University, Riyadh, Saudi Arabia

Correspondence should be addressed to Mashael Mohammed Bin-Meferij; mmbinmufayrij@pnu.edu.sa

Among the metallic nanoparticles (NPs), silver NPs are the leading anticancer nanoagents due to their physicochemical properties and inhibitory activities against different cancers. Many reports exhibited the cytotoxic effect of silver-NPs fabricated by cyanobacteria against various cancer cell lines. However, their lethal mechanisms have not been elucidated. The antiproliferative and cytotoxic effects of silver-NPs synthesized previously using *Nostoc Bahar M* (N-SNPs), and their associated mechanisms were evaluated in the solid Ehrlich ascites carcinoma (EAC) tumor-bearing mice model. Blood parameters, liver enzymes (alanine transaminase, aspartate aminotransferase, and alkaline phosphatase), lactate dehydrogenase, adenosine triphosphate, and oxidative stress markers, including glutathione, glutathione peroxidase, catalase, and malondialdehyde, were analyzed. In addition, the expression of pro- and antiapoptotic genes and proteins was screened utilizing quantitative real-time polymerase chain reaction and western blotting. N-SNPs significantly reduced tumor size in mice without affecting body weight and did not compromise liver function or alter blood parameters. Besides, N-SNPs negatively impact membrane integrity and metabolic activity and significantly enhance oxidative stress by causing an imbalance in antioxidant activity in tumor tissues. Intriguingly, N-SNPs-stimulated apoptosis signaling pathways via a combination of enhanced and suppressed responses of pro- and antiapoptotic genes and proteins. The cytotoxic activity and apoptosis effect of N-SNPs in tumor tissue could be attributed to the surge in reactive oxygen species production and depletion of antioxidant activity. Certainly, N-SNPs could provide robust antitumor agents against solid tumors.

1. Introduction

Cancer is a critical global health problem. It is one of the main noncommunicable disorders and is responsible for 18.1 million cases worldwide [1]. In 2020, 9.9% of US cancer cases accounted for hematological cancers, while solid tumors accounted for 90% of cancer cases [2]. Unlike hematological cancers, solid tumors have a structure similar to normal tissue, such as the parenchyma, which contains neoplastic cells and the surrounding stroma [3]. Many therapeutic strategies are used to mitigate solid tumor growth, such as surgery, chemotherapy, radiation therapy, and thermotherapy. Despite these conventional therapies demonstrating good anticancer potential, solid tumors are still the leading cause of death in cancer patients [4]. These treatment strategies are associated with complications such as multiple drug resistance, bone marrow loss, low biocompatibility and selectivity, and alopecia [5]. These adverse effects have necessitated the development and screening of new therapeutic products with anticancer activity that do not suffer from these limitations [6, 7]. The emergence of nanoscience has allowed for the development of several novel strategies to fight cancer and overcome the side effect of conventional therapies [8, 9]. Nanomaterials have been used successfully in therapeutics, diagnostics, cell imaging, labeling, and drug delivery in relation to cancer [10]. Many studies have shown

TABLE 1: Antibodies used in the current study.

Antibody	Type	Antibody dilution	Product code	Company
Bcl-2	Rabbit polyclonal	1 : 1,000	ab196495	Abcam
Bax	Rabbit monoclonal	1 : 1,000	ab232479	Abcam
Caspase 3	Rabbit monoclonal	1 : 1,000	Ab184787	Abcam
Caspase 9	Rabbit monoclonal	1 : 1,000	Ab202068	Abcam
Cleaved caspase 3	Rabbit monoclonal	1 : 1,000	Ab214430	Abcam
Cleaved caspase 9	Rabbit polyclonal	1 : 1,000	asp353	Cell Signaling Technology
Cytochrome c	Rabbit polyclonal	1 : 1,000	ab90529	Abcam
β-Actin	Rabbit monoclonal	1 : 1,000	ab115777	Abcam

that nanoparticles (NPs) resulted in a greater bioactivity against various types of cancer in vitro and in vivo [6, 11, 12].

Among metallic NPs, silver NPs (Ag-NPs) are relatively more useful in nanomedicine, mechanosensitive-based chemotherapies, immunotherapies, drug delivery, industry, and agriculture due to their physicochemical properties and biological activities [13, 14]. Silver NPs have been used recently in marketed products and medical applications due to their attractive biological activities [15]. Clinically, Ag-NPs are used in wound healing dressings such as KerraContact Ag and Acticoat Flex 7 and are also used to deliver medicines such as Doxil®/Caelyx and Abraxane®/ABI-007 [16–18]. Many studies have shown that Ag-NPs exert potent anticancer activity against the liver [12], breast [19], lung, and colon, etc., cancers [6, 20]. Furthermore, the large surface area to volume ratio of Ag-NPs allows for surface functionalization, which allows for better targeting and efficacy of therapeutic activity than many traditional anticancer drugs [21].

Different synthesis methods, including chemical, physical, and green approaches, are available to fabricate precursor materials into their NPs. Traditional chemical methods of NP production result in the accumulation of toxic materials on the surface of NPs, which can lead to cytotoxicity. Furthermore, the toxic chemicals used in these traditional methods can negatively impact the environment [22, 23]. Green synthesis of NPs requires natural resources such as cyanobacteria, algae, plants, fungi, and lichens, and naturally extracted biomolecules such as pigments, vitamins, polysaccharides, proteins, and enzymes to reduce bulk materials (the target metal salts) into a nanoscale product [24, 25]. Thus, biofabrication of NPs is a safer, eco-friendly, and relatively inexpensive alternative to conventional routes of production [22]. Many recent studies have used cyanobacteria as bio-factories for the synthesis of NPs, which demonstrated the natural capability of these bacteria for particle size reduction [11, 26]. *Nostoc* sp. is a novel species of cyanobacteria that spread in several niches such as soil and hot springs. They can survive in diverse and extreme environmental conditions, which facilitates their use as potent bioagents to eliminate heavy metal pollutants [27]. *Nostoc Bahar M* sp. has a variety of biocompunds, including cyclic and linear lipopeptides, fatty acids, alkaloids, and other organic chemicals. These biomolecules have a great reducing power to convert these heavy metals into nanosized metal nuclei [11, 28]. *Nostoc Bahar M* sp. is recently shown to be capable

of converting silver nitrate into Ag-NPs (referred to as N-SNPs) by Bin-Meferij and Hamida [11].

The mechanism of action of NPs against malignant cells is not fully understood [6]. One theory is that NPs exert anticancer activity via the production of reactive oxygen species (ROS), which results in intensive oxidative stress, leading to DNA damage, cell dysfunction, and cell death [14]. Some studies have suggested that NPs disrupt cellular structures such as membranes, nucleus, and organelles [29]. The molecular mechanisms of NPs remain unclear. However, studies have suggested that NPs may induce cell death by promoting various programed cell death such as apoptosis, necrosis, and autophagy [30]. Ag-NPs embedded in exopolysaccharides exerted cytotoxic effects against SKBR3 cells via ROS production, which induced cell death through apoptosis and autophagy [31]. Wilhelmi et al. [32] explored the mechanism of action of zinc oxide (ZnO)-NPs against RAW 264.7 macrophages. This study showed that ZnO-NPs induced rapid p47phox nicotinamide adenine dinucleotide phosphate oxidase-mediated superoxide radical generation, which resulted in oxidative DNA damage, necrosis, and caspase9/3-dependent apoptosis.

The present study evaluated the antitumor potentiality and explained the possible lethal mechanism of N-SNPs against EAC tumor-bearing mice model using biochemical, biological, and molecular assays. The results of our study indicated that N-SNPs might be a robust and potent candidate for cancer therapy.

2. Materials and Methods

2.1. Materials. EAC tumor-bearing mice were purchased from the Medical Research Institute, Alexandria, Egypt. All standard chemicals, glutathione peroxidase (GPx), and catalase (CAT) antioxidants were purchased from Sigma-Aldrich (St. Louis, MO, USA). The lactate dehydrogenase (LDH) (ab102526), alanine transaminase (ALT) (ab105134), aspartate aminotransferase (AST) (ab105135), alkaline phosphatase (ALP) (ab83369), glutathione (GSH) (ab239709), malondialdehyde (MDA) (ab233471), and adenosine triphosphate (ATP) assay kits (ab83355), and antibodies (Table 1) were purchased from Abcam (Cambridge, UK), while cleaved caspase 9 was purchased from Cell Signaling Technology (Danvers, USA).

2.2. Preparation of N-SNPs Suspension. Silver NPs were previously synthesized using *Nostoc Bahar M* sp. and characterized
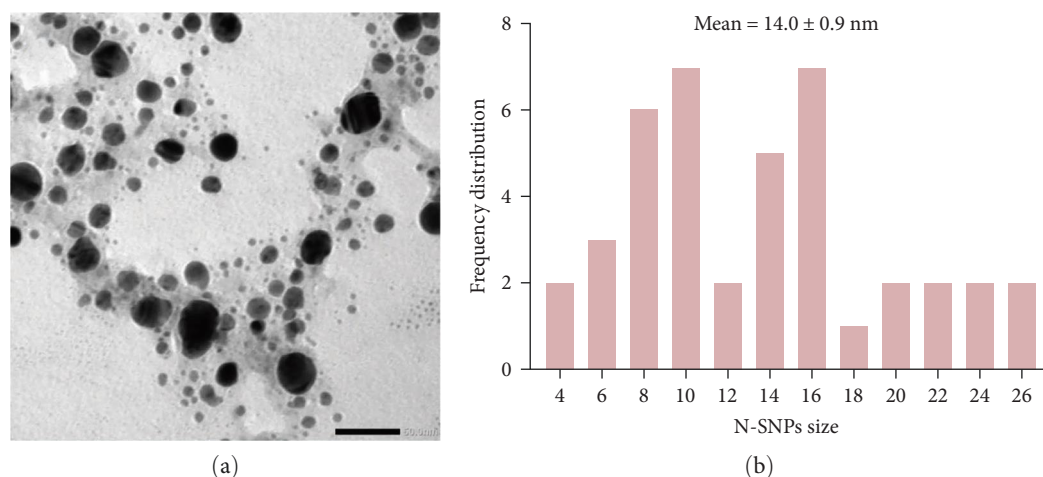
(a)

(b)

FIGURE 1: (a) TEM micrographs and frequency distribution graph (b) of Ag-NPs synthesized by *Nostoc Bahar M* sp. Scale bar of 50 nm.

TABLE 2: Animal groups for the *in vivo* study.

Groups	Refer to	EAC-tumor abundance	Oral administration
Group 1	Negative control	Absent	Saline
Group 2	Vehicle control	Present	Saline
Group 3	N-SNPs-treated groups	Present	85 μg/mouse of N-SNPs

using UV-spectrophotometry, X-ray diffraction, Fourier-transform infrared spectroscopy, and scanning and transmission electron microscopy by Bin-Meferij and Hamida [11]. N-SNPs had a quasispherical shape with a nanodiameter of 14.0 ± 0.9 nm (Figures 1(a) and 1(b)). For in vivo studies, 85 μg/mouse of N-SNPs was dissolved in 1 mL of distilled water for mice oral administration. The N-SNPs dose (85 μg/mouse) was chosen for in vivo studies based on a previous report [6, 11, 33].

2.3. Animal Study

2.3.1. Animal.
Eighteen male Balb/c mice (5–6 weeks old; 20–30 g) were randomly placed and allowed to acclimate, for 10 days, in polycarbonate cages with sawdust bedding prior to the initiation of the experiment. The animals were allowed access to food and water *ad libitum* at ambient temperature ($20 \pm 4°C$) (12 hr light/dark cycles). Animal handling, housing, and experimental design were approved by the Ethics Committee of Faculty of Medicine Alexandria University, Egypt (IRB NO: 0012098).

2.3.2. Ehrlich Ascites Carcinoma (EAC) Animal Model and Animal Grouping.
EAC suspension (10%; v/v) was prepared in normal sterile saline from fresh ascitic fluid collected from EAC bearing-donor mice (7–14-day-old EAC). EAC suspension (0.2 mL; 1×10^6 cells) was intravenously injected into the left hind thigh of the mice [34, 35]. When the tumors reached 2 cm^3, the mice were divided to equalize the mean tumor size among the groups. Eighteen male Balb/c mice were randomly divided into three groups (six animal/group), including group 1 (negative control group; normal mice have no tumors and orally administered saline daily), group 2 (vehicle control; EAC tumor-bearing mice orally administered saline daily), and group 3 (EAC tumor-bearing mice orally administered a daily dose of N-SNPs (85 μg/mouse) for 15 days). The experiment was performed in triplicate with 6 animals per group (total $n = 18$). the N-SNPs dose (85 μg/mouse) and experiment duration were chosen based on a previous study (Table 2) [36, 37].

2.3.3. Body Weight and Tumor Size Measurement.
The influence of N-SNPs on body weight (Bwt) and tumor size was estimated in all groups every 3 days of the duration of the experiment (15 days). The dimensions of tumors were evaluated using a digital caliper. Tumor size was calculated for vehicle control and N-SNPs-treated group using the formula $V = 0.52 \times L \times (W)^2$, where V is tumor volume, L is length, and W is width [38].

2.3.4. Hematologic Analysis.
Animals were fasted overnight, weighed, and anesthetized with diethyl ether at the end of the experiment. Blood samples from the retro-orbital venous plexus were collected into glass centrifuge tubes without anticoagulant via heparinized capillary tubes. The samples were incubated at ambient temperature to allow clotting to occur, then centrifuged at 3,000 rpm for 15 min. The sera were collected and kept at −20°C for biochemical experiments. Another set of blood samples was immediately added to ethylenediaminetetraacetic acid-coated vials for complete blood analysis using an automated hematologic analyzer (Mindray-bc-30s, Shenzhen, China) [33, 39].

2.3.5. EAC Tumor Sample Collection.
The mice were euthanized by cervical dislocation for the collection of EAC tumors

TABLE 3: Primers for qRT-PCR.

Gene	Primer	Reference
Bcl-2	F: CATGTGTGTGGAGAGCGTCAAC R: CAGATAGGCACCCAGGGTGAT	[42]
Bax	F: GTTTCA TCC AGG ATC GAG CAG R: CATCTT CTT CCA GAT GGT GA	[43]
Cytochrome c	F: TTTGGATCCAATGGGTGATGTTGAG R: CCATCCCTACGCATCCTTTAC	[44]
Caspase 3	F: TATGGTTTTGTGATGTTTGTCC R: TAGATCCAGGGGCATTGTAG	[42]
Caspase 9	F: TACAGCTGTTCAGACTCTAGTA R: AAATATGTCCTGGGGTAT	[42]
GAPDH	F: CCCTTCATTGACCTCAACTA R: TGGAAGATGGTGAT GGGATT	[43]

from each mouse in the vehicle control and N-SNPs-treated groups. The tumors were extracted and stored in 10% formalin for biochemical analyses, western blot, and quantitative real-time polymerase chain reaction (qRT-PCR) assays [33].

2.4. Biochemical Analyses. To assess the effects of N-SNPs on liver function, membrane integrity, and metabolic activity; liver enzymes (ALT; OD_{570}, AST; OD_{450}, and ALP; OD_{405}), LDH; OD_{490} and ATP; OD_{570}, respectively, were evaluated in the serum of all tested animal groups according to the kit manufacturer's instructions using a plate reader (Bio-Rad Laboratories, Hercules, CA, USA).

Oxidative stress markers (GSH; (OD_{412}), GPx (OD_{340}); CAT (OD_{520})) and a lipid peroxidation marker (MDA; OD_{532}) were analyzed in vehicle control and N-SNPs-treated group tissues as previously mentioned [6, 33, 40, 41]. In brief, the extracted EAC tumors were washed several times with ice-cold phosphate buffer saline and tissue lysates were prepared by homogenizing in lysis buffer (50 mM Tris, pH 7.5, 150 mM NaCl, 1% Triton X-100, 0.1% sodium dodecyl sulfate (SDS)). Lysates were centrifuged at 10,000 g at 4°C for 15 min and the supernatants were collected for GPx, CAT, GSH, and MDA according to the kit manufacturer's instructions using a plate reader. All analyses were repeated at least in triplicate under identical conditions.

2.5. qRT-PCR. To detect the influence of N-SNPs on gene expression in EAC tumor-bearing mice, five genes including Bcl-2, Bax, cytochrome c (Cyt c), caspase 3, and caspase 9 were analyzed using qRT-PCR before and after treatment mice groups with 85 μg/mouse of N-SNPs for 15 days. Briefly, a TRIzol reagent (Cat. No: 15596026, Life Technologies, United States) was used to extract the total RNA prior to the quality assessments of the extracted RNA. The quantity and quality of total RNA were estimated spectrophotometrically (UV 2505 spectrophotometer, Los Angeles, United States) according to the absorbance at 260 nm and the 260/280 nm ratio, respectively. The mRNA was detected using SYBR Green/ Fluorescein qPCR Master Mix and a Rotor-Gene Q instrument. QuantiTects Reverse Transcription Kit (Cat. No: 205311, Qiagen, Germantown, United States) with a random primer hexamer in a two-step RT-PCR was used for cDNA synthesis from the extracted RNA per manufacture

instructions. Genomic DNA contamination was eradicated using gDNA Wipeout Buffer. 30 ng cDNA was used as a template (final concentration = 300 nM) for amplification using specific primer pairs (Table 3). GAPDH (housekeeping gene) was used as a control gene. The threshold cycle (C_t) values of the investigated genes were normalized to the average C_t value of the control gene (ΔC_t), and the relative expression of each assessed gene using the 2–$\Delta\Delta C_t$ method (The Rotor-Gene Q, Qiagen, Germantown, United States) [6, 45].

2.6. Western Blotting. To explore the killing mechanistic pathway of N-SNPs in EAC tumors, seven pro- and anti-apoptotic proteins, including Bax, Bcl-2, pro- and activated caspase 3, pro- and activated caspase 9, and Cyt c were evaluated in untreated EAC tumors and EAC tumors treated with N-SNPs (85 μg/mouse) for 15 days using western blotting.

In brief, tissue lysates were prepared by homogenizing tumor tissues in lysis buffer (50 mM Tris, pH 7.5, 150 mM NaCl, 1% Triton X-100, 0.1% SDS) with protease inhibitors (Cat. No: ab65621, Abcam, Cambridge, UK) at 4°C for 30 min. Lysates were centrifuged at 10,000 g at 4°C for 15 min and the supernatants were collected. Protein concentration was estimated using the Bradford method [46]. Protein samples (30 μg) were loaded into mini-gel wells using a special gel loading tip, which was submerged in a migration buffer containing SDS. Then the gels were stained with 0.1% Coomassie blue R-250 for 2 hr, then destained with glacial acetic acid, then with methanol and water. Following SDS polyacrylamide gel electrophoresis, the proteins were transferred to a Hybond™ nylon membrane (GE Healthcare, New York, USA) using a TE62 standard transfer tank with a cooling chamber (Hoefer Inc. Holliston, Massachusetts, United States). Proteins were detected using primary antibodies (dilution range of 1 : 1,000) for each tested protein. All protein levels were normalized to β-actin. A gel documentation system (Geldoc-it UVP, Loughborough, Leicestershire, England) was used for data analysis with Total Lab analysis software (https://totallab.com/), version 1.0.1 [6].

2.7. Statistical Analysis. All analyses were performed at least three times independently, and data are presented as the mean ± standard error of the mean (SEM). Significant differences and the comparison between data (treated and untreated
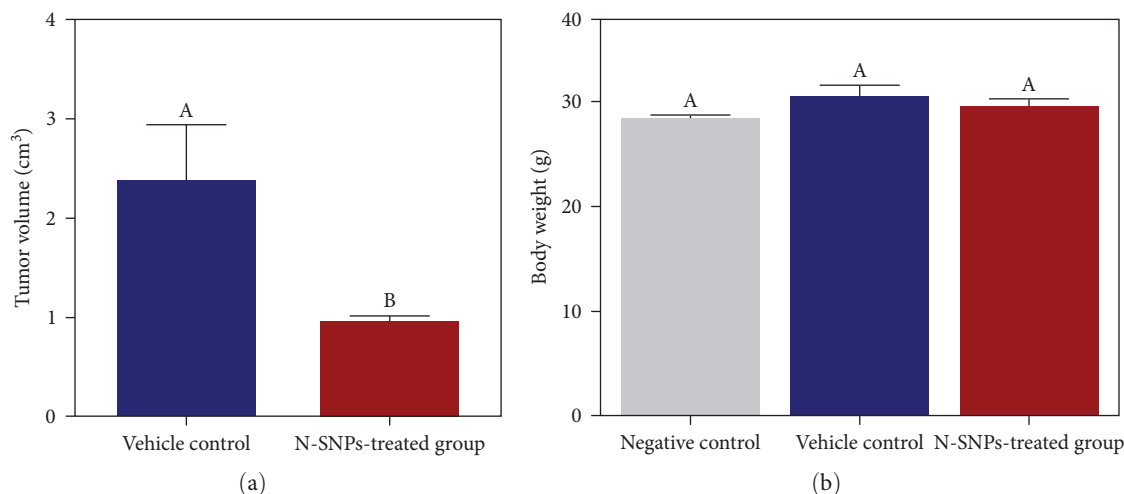
FIGURE 2: Effect of N-SNPs on (a) EAC tumor size and (b) body weights (Bwt) of negative control, vehicle control, and EAC bearing-tumor mice treated with 85 μg/mouse of N-SNPs for 15 days. Data represent at least three independent experiments and are reported as the mean ± SEM. Different letters refer to statistical significance at $p < 0.01$ (vehicle vs. N-SNPs-treated group), and the means with the same letter are not significantly different) based on the Mann–Whitney U test.

TABLE 4: Blood parameters.

Parameters	Negative control	Vehicle control	N-SNPs-treated group
WBCs ($\times 10^3/\mu$L)	4.8 ± 0.8^a	15.5 ± 3.0^{ab}	9.5 ± 0.9^b
RBCs ($\times 10^6/\mu$L)	9.1 ± 0.19^a	8.9 ± 0.2^a	8.7 ± 0.2^a
Hb (g/dL)	11.51 ± 0.25^a	11.8 ± 0.17^a	11.5 ± 1.0^a
HCT (%)	46.2 ± 0.8^a	41.6 ± 0.8^a	41.3 ± 1.8^a
MCV (fL)	50.8 ± 0.3^a	47 ± 0.9^a	47.9 ± 0.8^a
MCH (pg)	16.2 ± 0.03^a	15.3 ± 0.05^a	13.3 ± 0.3^a
MCHC (g/dL)	31.8 ± 0.1^a	28.4 ± 0.6^a	27.7 ± 0.2^a
RDW-CV (%)	20.3 ± 0.02^a	24.4 ± 2.1^a	23.9 ± 0.4^a
Platelets ($\times 10^3/\mu$L)	$1{,}249 \pm 14.7^a$	$1{,}139 \pm 64.1^a$	$1{,}281 \pm 70.4^a$
Neutrophil (%)	9.9 ± 1.8^a	21.43 ± 1.4^b	12.87 ± 2.9^{ab}
Lymphocytes (%)	36.9 ± 0.4^a	33.6 ± 2.2^a	45.5 ± 4.7^a
Monocytes (%)	11.5 ± 0.3^a	7.5 ± 2.5^a	16.73 ± 7.3^a
Eosinophil (%)	0.0 ± 0.0^a	0.03 ± 0.03^a	0.0 ± 0.0^a
Basophil (%)	19.2 ± 3.9^a	37.43 ± 1.56^a	19.47 ± 11.84^a
Ig ($\times 10^3/\mu$L)	0.1 ± 0.05^a	0.0 ± 0.0^a	0.03 ± 0.03^a

Data represent at least three independent experiments and are reported as the mean ± SEM. Different letters (a,b) refer to statistical significance at $p \leq 0.05$ (negative control significant vs. vehicle control and N-SNPs-treated groups) and the means with the same letter are not significantly different, as determined using one-way ANOVA analysis.

samples) were statistically determined using one- and two-way analysis of variance (ANOVA) or Mann–Whitney U test by using Prism 8.3 software (GraphPad Software Inc., La Jolla, CA, USA). Significance levels are presented at $p \leq 0.05$, $p = 0.001$, $p < 0.001$, and $p < 0.0001$.

3. Results

3.1. Influence of N-SNPs on Body Weight and Tumor Progression in Balb/c Mice.
The Bwts of the mice in the selected groups were estimated throughout the 15-day experiment. The data exhibited that mice of vehicle control showed a nonsignificant surge in Bwt (32.3 ± 1.0 g) compared to mice in the negative control (30 ± 0.3 g). This could be attributed to tumor burden [47]. While animals

treated with 85 μg/mice of N-SNPs showed a nonsignificant decrease in their Bwt (31.32 ± 0.7 g) compared to untreated EAC tumor-bearing mice group. Besides, the data of tumor sizes estimation throughout the 15-day experiment illustrated that N-SNPs resulted in a significant reduction in tumor size in N-SNPs-treated group (0.9914 ± 0.04 cm^3) compared with that in vehicle control (2.38 ± 0.56 cm^3) (Figure 2). These data indicated that N-SNPs significantly inhibit tumor progression without influencing Bwt of mice.

3.2. Haematological Parameters.
Comparative analysis of hematological parameters in the negative control, vehicle control, and N-SNPs treated groups is summarized in Table 4. The results demonstrated that the negative control
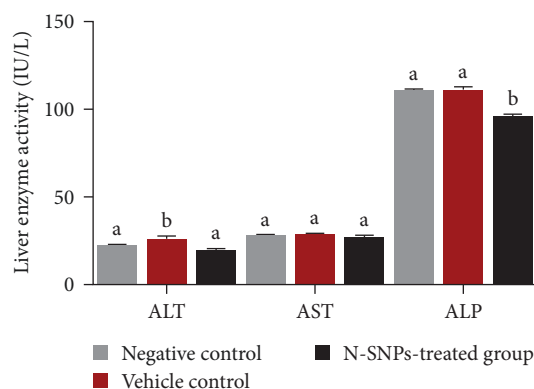
FIGURE 3: Alanine transaminase (ALT), aspartate aminotransferase (AST), and alkaline phosphatase (ALP) levels in serum of negative control, vehicle control, and EAC bearing-tumor mice treated with 85 μg/mouse of N-SNPs for 15 days. Data represent at least three independent experiments and are reported as the mean ± SEM. Different letters refer to statistical significance at $p < 0.001$ (for ALT) and $p < 0.0001$ (for ALP) (N-SNPs-treated group significant vs. vehicle control and negative control) and the means with the same letter are not significantly different based on one-way ANOVA analysis.

group had normal blood parameters. The vehicle control and N-SNPs-treated groups showed slight, but insignificant decreases in hematological parameters, including RBCs, Hb, HCT, MCV, MCHC, and MCH values compared with those in the negative control. The RDW-CV value in the vehicle control group (24.4% ± 2.1%) was greater than those in the negative control group (20.3% ± 0.02%) and the N-SNPs-treated group (23.9% ± 0.4%).

The vehicle control group had elevated WBC counts (15.5 ± 3.0 × 10³/μL) compared to those in the negative control group (4.8 ± 0.8 × 10³/μL), which may be attributed to tumor progression [39]. However, the N-SNPs-treated group (9.5 ± 0.9 × 10³/μL) showed a nonsignificant decrease in WBC number compared with that in the vehicle control group but still was higher than that in the negative control group. Neutrophil count was higher in the vehicle control group (21.43% ± 1.4%) than that in the negative control group (9.9% ± 1.8%) and N-SNPs-treated group (12.87% ± 2.9%). Lymphocytes were insignificantly increased (45.5% ± 4.7%) in the N-SNPs-treated group compared with that in the vehicle control group (33.6% ± 2.2%) and the negative control group (36.9% ± 0.4%). Monocyte numbers were insignificantly increased in the N-SNPs-treated group (16.73% ± 7.3%) compared with those in the vehicle control (7.5% ± 2.5%) and the negative control (11.5% ± 0.3%) groups. Eosinophils were not detected (0%) in both N-SNPs-treated group and negative control but its count in vehicle control groups was 0.03% ± 0.03%. Basophil count was higher in the vehicle control group (37.43% ± 1.56%) than that in the negative control group (19.2% ± 3.9%) and in the N-SNPs-treated group (19.47% ± 11.84%). No other parameters were significantly different between the N-SNPs-treated and the negative control groups, and any marginal differences were represented by values in the normal range.

3.3. Effect of N-SNPs on Liver Function.
The toxic effect of 85 μg/mice N-SNPs on liver function was evaluated by measuring the level of liver enzymes, including ALT, AST, and ALP in the sera of negative control, vehicle control, and N-SNPs-treated groups after 15 days. The data revealed that the mice of vehicle control showed a significant increase in ALT level (25.29 ± 1.3 IU/L) compared with mice in the negative control group (22.28 ± 0.38 IU/L). While N-SNPs treatment caused a significant dropping in ALT level of N-SNPs-treated group mice (19.37 ± 0.76 IU/L) compared to the vehicle control group and a nonsignificant decrease compared to that in the negative control group. Moreover, vehicle control groups showed no change in their AST and ALP levels with values of 28.2 ± 0.2 and 111.3 ± 1.1 IU/L compared to that in negative control with the value of 28 ± 0.7 and 111.2 ± 0.3 IU/L, respectively. However, N-SNPs treatment caused a non-significant decrease in AST level (27.3 ± 0.6 IU/L) and a significant drop in ALP level (95.8 ± 1.2 IU/L) compared with negative control and vehicle control groups (Figure 3).

3.4. Membrane Integrity and Metabolic Toxicity.
The influence of 85 μg/mice N-SNPs on the membrane integrity of tumor cells was estimated by measuring the LDH level in sera of negative control, vehicle control, and N-SNPs-treated groups. The results exhibited that N-SNPs treatment significantly reduced the LDH level of N-SNPs-treated mice (865.1 ± 13.3 μmol/mL) compared with negative control and untreated vehicle control group (911 ± 0.9 and 923 ± 1.6 μmol/mL, respectively). The toxic effect of 85 μg/mice N-SNPs on metabolic activity in tumor tissue was evaluated by estimating ATP levels in sera of negative control, vehicle control, and N-SNPs-treated groups. The data showed that ATP levels did not significantly change in the three tested groups. ATP level of N-SNPs-treated group was 1.5 ± 0.1 μmol/mL, while in the vehicle control group and negative control group was 1.55 ± 0.02 and 1.5 ± 0.008 μmol/mL, respectively (Figure 4). These data revealed that N-SNPs might have no direct negative impacts on mitochondrial function.

3.5. Antioxidative Markers.
The potentiality of 85 μg/mice N-SNPs to induce oxidative stress in tumor tissue via promoting ROS formation was estimated by analyzing GSH, GPx, CAT, and MDA levels in the vehicle control group and N-SNPs-treated group tissues. The data demonstrated that N-SNPs caused a nonsignificant but slight decrease in GSH level and a significant reduction in CAT level of the N-SNPs-treated group (45.1 ± 1.6 nmol/mg protein and 2.88 ± 0.08 μg/g protein, respectively) in comparison with the vehicle control group (46.29 ± 0.8 nmol/mg protein and 3.55 ± 0.08 μg/g protein, respectively). In addition, the N-SNPs-treated group revealed a significant surge in GPx level and a nonsignificant increase in MDA level with a value of 87.24 ± 1.2 nmol/mg protein and 9.83 ± 0.9 μM/g protein, respectively) in comparison with the vehicle control group (73.6 ± 0.8 nmol/mg protein and 8.9 ± 0.1 μM/g protein, respectively) (Figure 5). These results revealed that N-SNPs
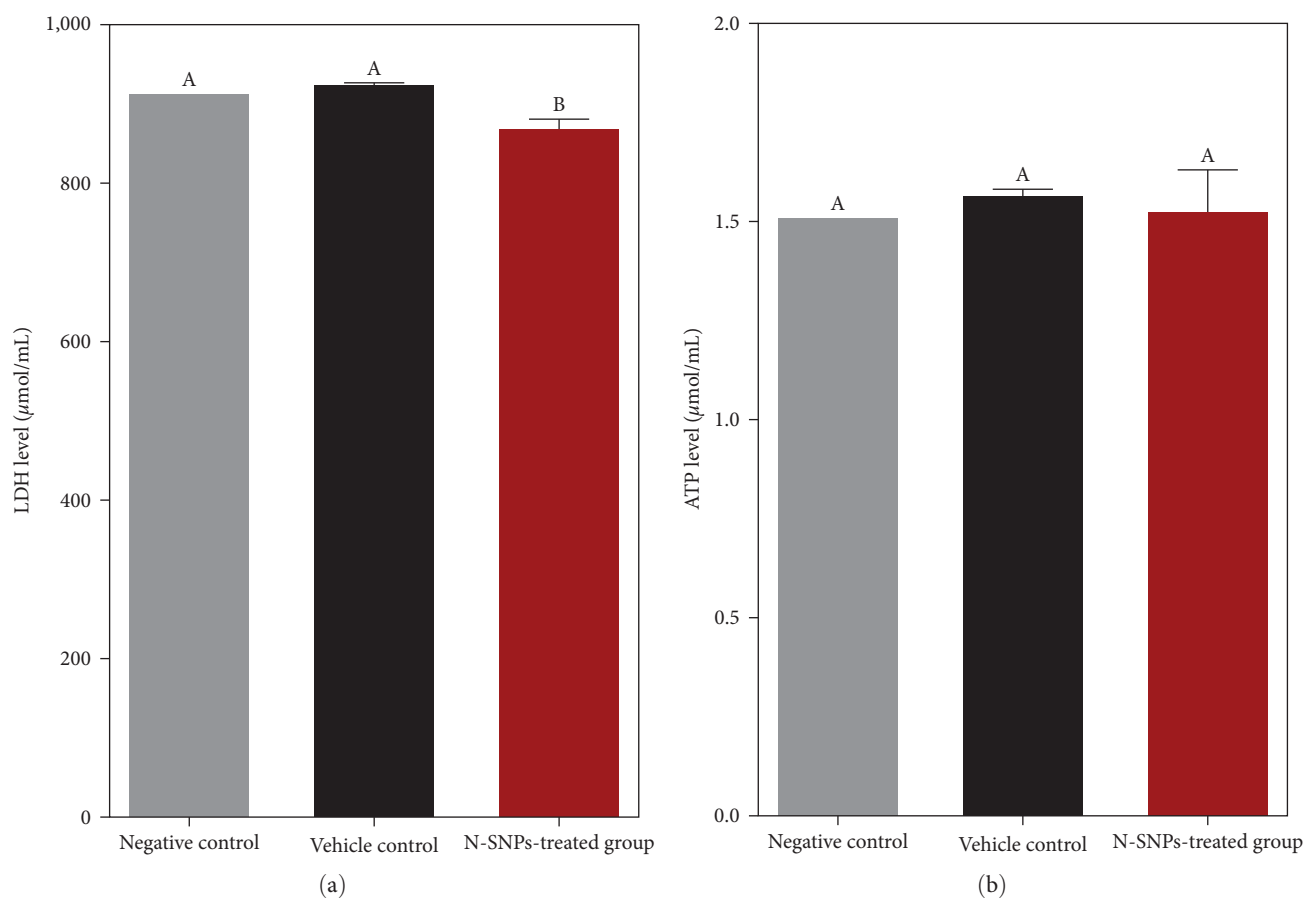
(a)

(b)

FIGURE 4: Lactate dehydrogenase (LDH) (a) and adenosine triphosphate (ATP) (b) levels in sera of negative control, vehicle control, and EAC tumor-bearing mice treated with 85 μg/mouse of N-SNPs for 15 days. Data represent at least three independent experiments and are reported as the mean $\pm$ SEM. Different letters refer to statistical significance at $p < 0.0001$ (N-SNPs-treated group significant vs. negative control and vehicle control) and the means with the same letter are not significantly different based on one-way ANOVA analysis.

induced oxidative stress inside malignant cells by enhancing ROS formation and influencing antioxidant activities resulting in apoptosis.

3.6. Influence of N-SNPs on Gene Expression. To further investigate the mechanism of action of N-SNPs against EAC tumors, five pro- and antiapoptotic genes were screened using qRT-PCR. The data revealed that EAC tumor-bearing mice subjected to N-SNPs (85 μg/mouse) for 15 days exhibited a nonsignificant downregulation of Bcl-2 gene expression, while a nonsignificant upregulation of Bax, Cyt c, caspase 3, and the significant surge in caspase 9 gene expression level compared with gene expression levels in the vehicle control group (Figure 6). These results suggested that N-SNPs enhance the intrinsic apoptosis signaling pathway inside EAC-tumor tissues.

3.7. Influence of N_SNPs on Protein Expression. The lethal mechanism of 85 μg/mouse N-SNPs against EAC tumors was examined by analyzing the antiapoptotic and apoptotic proteins expression using a western blot assay. The data revealed that EAC tumor-bearing mice that received oral N-SNPs for 15 days had significantly decreased expression levels of Bcl-2 protein compared with those in the vehicle

control group. On the contrary, treatment with N-SNPs enhanced a nonsignificant upregulation of Bax, procaspase 9, Cyt c, and a significant increase in procaspase 3, activated caspase 3, and activated caspase 9 protein expression levels compared with those in the vehicle control group (Figure 7). These results highlighted that N-SNPs may induce intrinsic apoptosis inside EAC-tumor tissue.

4. Discussion

The potential of N-SNPs to suppress tumor progression and the molecular mechanisms of the antiproliferative effects of N-SNPs were investigated in an EAC-induced allograft mouse tumor model. Herein, we choose the time of exposure (15 days) for N-SNPs based on previous literature that reported the biocompatibility of this duration on animal parameters, including hematological, physiological, and histological parameters. Many investigations reported that animal groups exposed to biogenic Ag-NPs for 15 days did not show any toxicity on animal physiological parameters, organs (such as liver), and their functions, but the long exposure and higher concentration of Ag-NPs may be caused systematic toxicity [48]. On the other hand, other scholars reported that treatment EAC tumor-bearing mice with
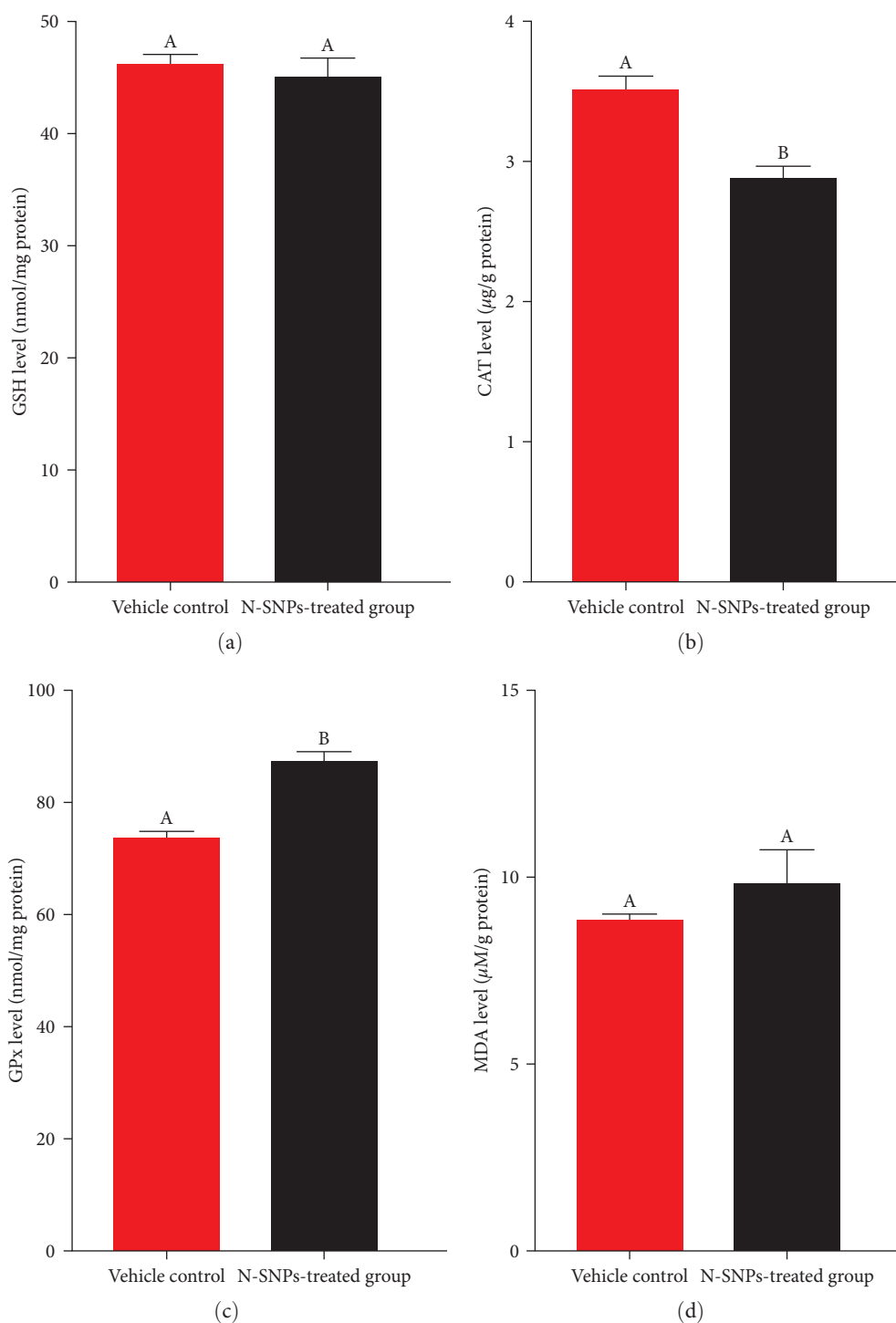
FIGURE 5: (a) Glutathione (GSH), (b) glutathione peroxidase (GPx), (c) catalase (CAT), and (d) malondialdehyde (MDA) levels in tumor tissue of EAC tumor-bearing mice (vehicle control), and EAC tumor-bearing mice treated with $85\,\mu g$/mouse of N-SNPs for 15 days. Data represent at least three independent experiments and are reported as the mean $\pm$ SEM. Different letters refer to statistical significance at $p < 0.0001$ (N-SNPs-treated group significant vs. vehicle control) and the means with the same letter are not significantly different based on the Mann–Whitney U test.

biogenic Ag/AgCl-NPs for 20 days showed a reduction in their tumor size while their lifespan increased by 75% compared to untreated EAC tumor-bearing mice [35]. El-Naggar et al. [49] reported that 5 mg/kg Bwt of Ag-NPs synthesized by *Nostoc linckia* pigment exhibited a significant reduction in tumor size of EAC tumor-bearing mice (1.3 ± 1.2 mL) compared to untreated EAC tumor-bearing mice (7.5 ± 1.8 mL) and that treated with 5 mg/kg Bwt of 5 FU (1.5 ± 0.6 mL) with decreasing their Bwt. El-Sonbaty et al. [50] reported that female EAC tumor-bearing mice treated with 0.1, 1.0,
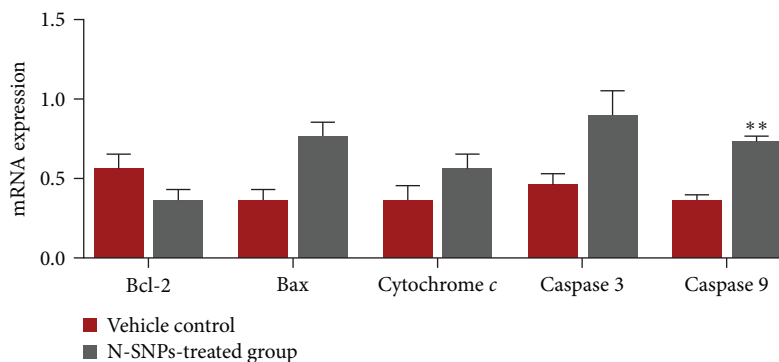
FIGURE 6: Influence of N-SNPs (85 μg/mouse) on Bcl-2, Bax, cytochrome *c*, caspase 3, and 9 gene expression levels in EAC tumor-bearing mice. All data represent at least three independent experiments and are reported as the mean ± SEM. *p*-values were measured versus untreated EAC tumor-bearing mice (vehicle control): $^{**}p = 0.001$ based on the Mann–Whitney *U* test.
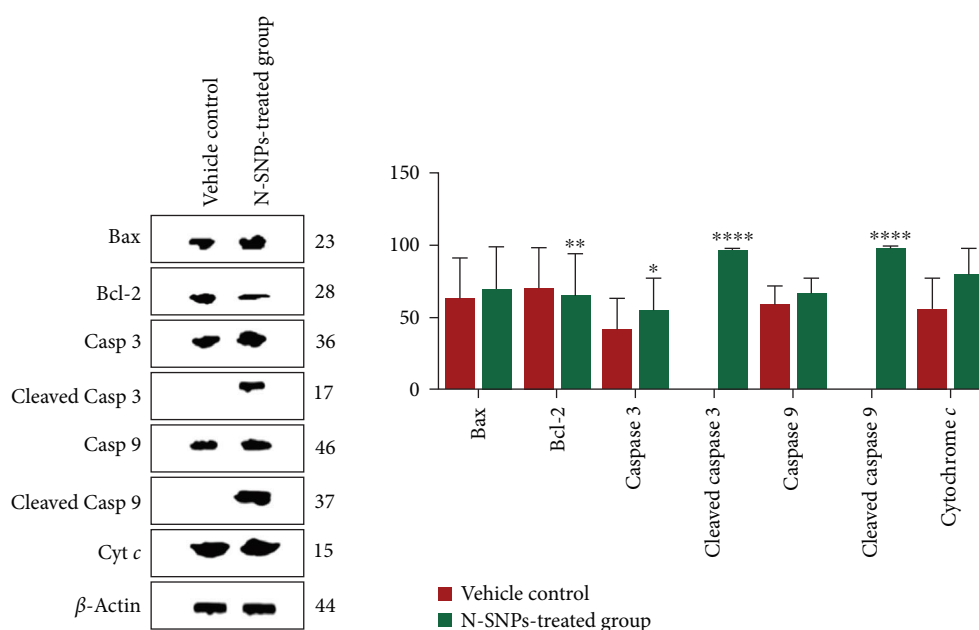

FIGURE 7: Influence of N-SNPs (85 μg/mouse) on antiapoptotic (Bcl-2) and proapoptotic (Bax, caspases 3, 9, and cleaved caspase 3, cleaved caspase 9, and cytochrome *c*) protein expression levels in EAC tumor-bearing mice. All data represent at least three independent experiments and are presented as the mean ± SEM. *p*-values were measured versus untreated EAC tumor-bearing mice group (vehicle control): $^{*}p \leq 0.05$, $^{**}p < 0.001$ and $^{****}p < 0.0001$ based on the Mann–Whitney *U* test.

and 10 μg/kg of Ag-NPs by i.p. for 15 days showed no abnormalities or any symptoms of toxicity. El Bialy et al. [33] showed that EAC tumor-bearing mice treated with 42.5 and 85 μg/mice of Ag-NPs synthesized using *Turbinaria turbinata* for 20 days resulted in a decrease in Bwt and tumor size of mice compared with untreated EAC tumor-bearing group suggesting that biogenic Ag-NPs represented potent antitumor agents with limited adverse effects.

Hematological analysis showed that N-SNPs did not cause any significant change in RBCs, Hb, HCT, MCV, MCH, MCHC, RDW-CV, and platelets levels compared with those in the normal mice (negative control), and EAC tumor-bearing mice group (vehicle control), which highlighted that N-SNPs did not induce systemic toxicity [39, 51]. Treatment with N-SNPs resulted in decreased WBCs count in the N-SNPs-treated group compared with

those in the vehicle control groups and an increase in lymphocyte and monocyte counts in the N-SNPs-treated group compared with those in the negative control and vehicle control groups, which may indicate that N-SNPs induced an immune response to suppress tumor proliferation [52].

The liver enzymes ALT, AST, and ALP are essential markers of liver dysfunction. Increased ALT and AST levels indicate parenchymal cell damage, and abnormal ALP levels indicate cholestasis or infiltrative liver disease [53]. Our results showed that N-SNPs significantly decreased ALT and ALP levels and did not cause a significant change in AST levels in the N-SNPs-treated group compared to that in the vehicle control group. However, ALT, AST, and ALP levels after N-SNPs treatment were in the normal range, which indicated that N-SNPs did not induce severe liver toxicity [33]. Ashajyothi et al. [54] reported that mice groups

that received a dose range of 11–16 μg/kg (i/v) and 24–30 μg/kg (i/p) of biogenic ZnO NPs after 28 days showed a nonsignificant change in ALT, serum AST level and ALP level, which were 40.7 mg/dL, 37.9 and 82.4 IU/L normals as compared to control. Medhat et al. [55] showed that ALT and AST levels in sera of EAC tissue and solid tumor tissue of mice group were significantly increased, while after 10–12 days of gold-dextran NPs treatment, the level of both ALT and AST was highly dropped compared with untreated groups [55].

Blood biochemistry data showed that treatment N-SNPs resulted in significantly decreased LDH levels in the sera of the N-SNPs-treated group compared with those in the vehicle control group. Mohammed et al. [56] reported that EAC tumor-bearing mice showed significantly increased LDH levels (2,287 ± 132 U/L) of animal sera compared to those in a negative control group (1,620 ± 103 U/L), and LDH levels were significantly decreased in response to treatment with sulfur NPs (1,622 ± 77 U/L) in comparison to the EAC tumor-bearing group (vehicle control).

The data showed that the ATP level in N-SNPs-treated group was similar to that in the negative control and vehicle control groups. These results suggested that N-SNPs did not interfere with mitochondrial activity or ATP synthesis. Abdel-Gawad et al. [41] reported that ATP levels decreased in EAC tumor-bearing mice treated with calcium phosphate composite NPs.

GSH, GPx, and CAT are critical antioxidant molecules that can participate in the metabolism and clearance of ROS in tumor cells [57]. Studies have shown that decreased GSH levels in tumor cells resulted in a loss of tumor features such as cell division, mitochondrial biogenesis, and cell membrane integrity [58, 59]. GSH levels showed a slight but nonsignificant decrease in the N-SNPs-treated group compared to the vehicle control group, while the level of GPx was increased, and CAT level was decreased in N-SNPs-treated group. These data indicated that N-SNPs enhanced the formation of ROS and induced oxidative stress in tumor tissues, resulting in the inhibition of tumor progression. A recent study exhibited that biogenic Ag-NPs (average nanodiameter of 14.9 ± 0.56 nm) caused a significant surge in GPx level of MCF-7, HepG2, and HCT-116 cell lines, inducing oxidative stress [6]. Tunçsoy et al. [60] reported that copper oxide NPs (size <50 nm) caused a significant decrease in CAT and SOD levels and surged GPx level of gill and liver tissues of *Oreochromis niloticus* as a defense strategy against hydroperoxides caused by NPs. Abosharaf et al. [37] reported that GSH and CAT levels were significantly decreased in the EAC tumor-bearing mice group following the treatment with Ag-NPs that were synthesized using mango leaves extract.

The increase in MDA levels in tissue of the N-SNPs-treated group compared to those in vehicle control indicated that N-SNPs enhanced lipid peroxidation. Enhanced lipid peroxidation in response to N-SNPs may have been a result of the ability of N-SNPs to induce the production of ROS species that interact with fatty acids to form unstable lipid radicals [33]. El-Sonbaty [50] found that EAC bearing-mice treated with biogenic Ag-NPs (8–20 nm) and exposed to

gamma radiation revealed a significant surge in MDA level in their tumor tissue. The authors suggested that the inhibition of antioxidant activity enhanced lipid peroxidation.

Apoptosis can occur through two main pathways: the extrinsic, or death receptor, pathway, and the intrinsic, or mitochondria-dependent, pathway. In the intrinsic pathway, nonreceptor-mediated stimuli such as radiation or hypoxia induce apoptosis. These stimuli influence the inner mitochondrial membrane (IMM), resulting in the release of Cyt c into the cytoplasm. Cyt c binds to Apaf-1, which results in the activation of procaspase 9 and the formation of apoptosomes. The clustering of procaspase 9 promotes the production of caspase 9 and caspase 3, which results in the induction of apoptosis. Many studies have shown that Bcl-2 family members are important in regulating apoptosis. They modulate and control the intrinsic pathway by regulating IMM permeability. The Bcl-2 family can be divided into two groups. The first includes proteins that enhance apoptosis, such as Bax. The second group includes proteins that suppress apoptosis, such as Bcl-2. Our study showed that N-SNPs induced overexpression of a proapoptotic protein (Bax) and reduced the expression levels of Bcl-2, suggesting that EAC tumors treated with N-SNPs favored apoptosis. Yuan et al. [45] studied the lethal influence of Ag-NPs only and combined Ag-NPs with camptothecin (CTP), a telomerase inhibitor, and their possible mechanism against Hela cell lines. The authors found that Ag-NPs-CTP caused a significant decrease in Bcl-2 and a significant surge in Bax gene expression compared to Ag-NPs alone, suggesting that Ag-NPs-CTP induce apoptosis in Hela cells. In addition, our study showed that N-SNPs induced significant upregulation of apoptotic factors such as caspases 3, and 9, Cyt c, and Bax, and induced downregulation of the antiapoptotic Bcl-2 protein and gene. These results highlighted that N-SNPs may induce intrinsic apoptosis pathways in tumor tissue [61]. Kabir et al. [35] exhibited that biogenic Ag/AgCl-NPs caused a significant decrease in Bcl-2 protein expression level and a significant surge in cleaved caspase 3 and 9 in MCF-7 cells. The authors suggested that Ag-NPs treatment activated the caspases involved in intrinsic pathways resulting in cell death. Bhowmik et al. [62] showed that Au-NPs conjugated with snake venom protein toxin NKCT1 (Au-NPs-NKCT1) resulted in a significant upregulation in Bax, caspase 3 and 9 expressions and downregulation in Bcl-2 levels confirming that Au-NPs-NKCT1 stimulated the caspase-dependent apoptosis pathway in EAC cells. Jang et al. [63] reported that biogenic Ag-NPs induce apoptosis through the intrinsic pathway. Nakkala et al. [64] reported that Ag-NPs biosynthesized using *Ficus religiosa* leaf extract were able to upregulate both caspase 8 and 9 in lung cancer cell lines A549 and human epidermoid carcinoma cell line Hep2, enhancing apoptosis by extrinsic and intrinsic pathways. To sum up, N-SNPs showed great antiproliferative activity against EAC-tumor via enhancing the apoptosis signaling pathway.

5. Conclusion

The findings of this study shed novel insights on the antitumor activity and the mechanism underlying the lethal effects

of biogenic Ag-NPs previously synthesized using *Nostoc Bahar M* sp. (N-SNPs) against EAC tumor-bearing mice. The data showed that treatment mice groups with $85 \mu g$/mice of N-SNPs for 15 days significantly reduced tumor size without influence on Bwt of mice and did not induce severe liver toxicity, as evidenced by normal levels of the liver enzymes ALT, AST, and ALP, and also did not exhibit systemic toxicity, as evidence by normal blood parameters. N-SNPs led to a depletion in LDH and no change in ATP levels, suggesting that N-SNPs have no impacts on membrane integrity and metabolic activity of tumor tissue. N-SNPs stimulate intensive oxidative stress which was mainly mediated by modulation of CAT and GPx expression in tumor tissue and surge various proapoptotic genes and proteins expression and decrease antiapoptotic gene and protein expression, suggestive of their ability to negatively affect tumor progression via enhancing apoptosis pathways. The results indicated that the lethal effects of N-SNPs against tumor cells involved indirect effects, which included enhancing ROS production, leading to severe oxidative stress and, consequently, biomolecule dysfunction, structural damage to cells, and, ultimately, apoptosis. More studies need to be performed to evaluate the influence of long exposure of N-SNPs after different periods of treatment in vivo systems and optimize the suitable time of exposure, size, and concentration of Ag-NPs to reduce the side effects associated with these NPs. Furthermore, synergistic effects of N-SNPs with currently marketed anticancer drugs may also prove beneficial.

Abbreviations

NPs: Nanoparticles
SNPs: Silver nanoparticles
PCR: Polymerase chain reaction
nm: Nanometer
min: Minute
μL: Microliter
mg: Milligram
mL: Milliliter
μg: Microgram
rpm: Revolutions per minute.

Data Availability

The data supporting this article are available in Figures 1–7 and Tables 1–4. The data sets analyzed in the present study are available from the corresponding author upon reasonable request.

Ethical Approval

The study was conducted according to the guidelines of the Declaration of AAALAC and approved by the Ethics committee of Faculty of Medicine Alexandria University, Egypt (IRB No.: 0012098).

Conflicts of Interest

The authors declare that they have no conflicts of interest.

Authors' Contributions

Conceptualization: Reham Samir Hamida; methodology: Reham Samir Hamida and Mashael Mohammed Bin-Meferij; software: Reham Samir Hamida; validation: Reham Samir Hamida and Mashael Mohammed Bin-Meferij; formal analysis: Reham Samir Hamida; investigation: Mashael Mohammed Bin-Meferij and Reham Samir Hamida; writing—original draft preparation: Reham Samir Hamida; writing—review and editing: Reham Samir Hamida; visualization: Reham Samir Hamida; supervision: Mashael Mohammed Bin-Meferij; project administration: Reham Samir Hamida; funding acquisition: Mashael Mohammed Bin-Meferij and Gadah Albasher. All authors contributed to manuscript revision, read, and approved the submitted version.

Funding

References

[1] F. Bray, J. Ferlay, I. Soerjomataram, R. L. Siegel, L. A. Torre, and A. Jemal, "Global cancer statistics 2018: GLOBOCAN estimates of incidence and mortality worldwide for 36 cancers in 185 countries," *CA: A Cancer Journal for Clinicians*, vol. 68, no. 6, pp. 394–424, 2018.

[2] R. L. Siegel, K. D. Miller, A. Goding Sauer et al., "Colorectal cancer statistics, 2020," *CA: A Cancer Journal for Clinicians*, vol. 70, no. 3, pp. 145–164, 2020.

[3] Y. Liu, J. Zhou, Q. Li et al., "Tumor microenvironment remodeling-based penetration strategies to amplify nanodrug accessibility to tumor parenchyma," *Advanced Drug Delivery Reviews*, vol. 172, pp. 80–103, 2021.

[4] P. P. Nayak, S. Nijil, A. Narayanan, A. K. Badekila, and S. Kini, "Nanomedicine in cancer clinics: are we there yet?" *Current Pathobiology Reports*, vol. 9, pp. 43–55, 2021.

[5] J. Zugazagoitia, C. Guedes, S. Ponce, I. Ferrer, S. Molina-Pinelo, and L. Paz-Ares, "Current challenges in cancer treatment," *Clinical Therapeutics*, vol. 38, no. 7, pp. 1551–1566, 2016.

[6] R. S. Hamida, G. Albasher, and M. M. Bin-Meferij, "Oxidative stress and apoptotic responses elicited by *Nostoc*-synthesized silver nanoparticles against different cancer cell lines," *Cancers*, vol. 12, no. 8, Article ID 2099, 2020.

[7] S. Nirgude, R. Mahadeva, J. Koroth et al., "ST09, a novel curcumin derivative, blocks cell migration by inhibiting matrix metalloproteases in breast cancer cells and inhibits tumor progression in eac mouse tumor models," *Molecules*, vol. 25, no. 19, Article ID 4499, 2020.

[8] Q. Chen, G. Liu, S. Liu et al., "Remodeling the tumor microenvironment with emerging nanotherapeutics," *Trends in Pharmacological Sciences*, vol. 39, no. 1, pp. 59–74, 2018.

[9] A. I. Matos, B. Carreira, C. Peres et al., "Nanotechnology is an important strategy for combinational innovative chemo-immunotherapies against colorectal cancer," *Journal of Controlled Release*, vol. 307, pp. 108–138, 2019.

[10] C. Jin, K. Wang, A. Oppong-Gyebi, and J. Hu, "Application of nanotechnology in cancer diagnosis and therapy – a mini-review," *International Journal of Medical Sciences*, vol. 17, no. 18, pp. 2964–2973, 2020.

[11] M. M. Bin-Meferij and R. S. Hamida, "Biofabrication and antitumor activity of silver nanoparticles utilizing novel Nostoc sp. Bahar M," *International Journal of Nanomedicine*, vol. 14, pp. 9019–9029, 2019.

[12] H. Tang, C. Li, Y. Zhang et al., "Targeted manganese doped silica nano GSH-cleaner for treatment of liver cancer by destroying the intracellular redox homeostasis," *Theranostics*, vol. 10, no. 21, pp. 9865–9887, 2020.

[13] V. Jaishree and P. D. Gupta, "Nanotechnology: a revolution in cancer diagnosis," *Indian Journal of Clinical Biochemistry*, vol. 27, pp. 214–220, 2012.

[14] G. Raja, Y.-K. Jang, J.-S. Suh, H.-S. Kim, S. H. Ahn, and T.-J. Kim, "Microcellular environmental regulation of silver nanoparticles in cancer therapy: a critical review," *Cancers*, vol. 12, no. 3, Article ID 664, 2020.

[15] R. S. Hamida, M. A. Ali, A. Redhwan, and M. M. Bin-Meferij, "Cyanobacteria – a promising platform in green nanotechnology: a review on nanoparticles fabrication and their prospective applications," *International Journal of Nanomedicine*, vol. 15, pp. 6033–6066, 2020.

[16] V. C. Mazurak, R. E. Burrell, E. E. Tredget, M. T. Clandinin, and C. J. Field, "The effect of treating infected skin grafts with Acticoat™ on immune cells," *Burns*, vol. 33, no. 1, pp. 52–58, 2007.

[17] J. Boateng and O. Catanzano, "Advanced therapeutic dressings for effective wound healing—a review," *Journal of Pharmaceutical Sciences*, vol. 104, no. 11, pp. 3653–3680, 2015.

[18] D. Bobo, K. J. Robinson, J. Islam, K. J. Thurecht, and S. R. Corrie, "Nanoparticle-based medicines: a review of FDA-approved materials and clinical trials to date," *Pharmaceutical Research*, vol. 33, no. 10, pp. 2373–2387, 2016.

[19] N. I. Zulkifli, M. Muhamad, N. N. M. Zain et al., "A bottom-up synthesis approach to silver nanoparticles induces anti-proliferative and apoptotic activities against MCF-7, MCF-7/TAMR-1 and MCF-10A human breast cell lines," *Molecules*, vol. 25, no. 18, Article ID 4332, 2020.

[20] M. Rozalen, M. Sánchez-Polo, M. Fernández-Perales, T. J. Widmann, and J. Rivera-Utrilla, "Synthesis of controlled-size silver nanoparticles for the administration of methotrexate drug and its activity in colon and lung cancer cells," *RSC Advances*, vol. 10, no. 18, pp. 10646–10660, 2020.

[21] P. N. Navya, A. Kaphle, S. P. Srinivas, S. K. Bhargava, V. M. Rotello, and H. K. Daima, "Current trends and challenges in cancer management and therapy using designer nanomaterials," *Nano Convergence*, vol. 6, Article ID 23, 2019.

[22] P. Khanna, A. Kaur, and D. Goyal, "Algae-based metallic nanoparticles: synthesis, characterization and applications," *Journal of Microbiological Methods*, vol. 163, Article ID 105656, 2019.

[23] R. S. Hamida, M. A. Ali, N. E. Abdelmeguid, M. I. Al-Zaban, L. Baz, and M. M. Bin-Meferij, "Lichens—a potential source for nanoparticles fabrication: a review on nanoparticles biosynthesis and their prospective applications," *Journal of Fungi*, vol. 7, no. 4, Article ID 291, 2021.

[24] N. Asmathunisha and K. Kathiresan, "A review on biosynthesis of nanoparticles by marine organisms," *Colloids and Surfaces B: Biointerfaces*, vol. 103, pp. 283–287, 2013.

[25] A. Gour and N. K. Jain, "Advances in green synthesis of nanoparticles," *Artificial Cells, Nanomedicine, and Biotechnology*, vol. 47, no. 1, pp. 844–851, 2019.

[26] V. Patel, D. Berthold, P. Puranik, and M. Gantar, "Screening of cyanobacteria and microalgae for their ability to synthesize silver nanoparticles with antibacterial activity," *Biotechnology Reports*, vol. 5, pp. 112–119, 2015.

[27] J. M. Jacob, R. Ravindran, M. Narayanan, S. M. Samuel, A. Pugazhendhi, and G. Kumar, "Microalgae: a prospective low cost green alternative for nanoparticle synthesis," *Current Opinion in Environmental Science & Health*, vol. 20, Article ID 100163, 2021.

[28] B. Nowruzi, R.-A. Khavari-Nejad, K. Sivonen, B. Kazemi, F. Najafi, and T. Nejadsattari, "Identification and toxigenic potential of a Nostoc sp." *Algae*, vol. 27, no. 4, pp. 303–313, 2012.

[29] C.-G. Liu, Y.-H. Han, R. K. Kankala, S.-B. Wang, and A.-Z. Chen, "Subcellular performance of nanoparticles in cancer therapy," *International Journal of Nanomedicine*, vol. 15, pp. 675–704, 2020.

[30] R. Mohammadinejad, M. A. Moosavi, S. Tavakol et al., "Necrotic, apoptotic and autophagic cell fates triggered by nanoparticles," *Autophagy*, vol. 15, no. 1, pp. 4–33, 2019.

[31] M. Buttacavoli, N. N. Albanese, G. Di Cara et al., "Anticancer activity of biogenerated silver nanoparticles: an integrated proteomic investigation," *Oncotarget*, vol. 9, no. 11, pp. 9685–9705, 2018.

[32] V. Wilhelmi, U. Fischer, H. Weighardt et al., "Zinc oxide nanoparticles induce necrosis and apoptosis in macrophages in a p47phox- and Nrf2-independent manner," *PLoS ONE*, vol. 8, no. 6, Article ID e65704, 2013.

[33] B. E. El Bialy, R. A. Hamouda, K. S. Khalifa, and H. A. Hamza, "Cytotoxic effect of biosynthesized silver nanoparticles on Ehrlich ascites tumor cells in mice," *International Journal of Pharmacology*, vol. 13, no. 2, pp. 134–144, 2017.

[34] A. T. Ellethy, "Potential antitumor activity of nonsteroidal anti-inflammatory drugs against Ehrlich ascites carcinoma in experimental animals," *International Journal of Health Sciences*, vol. 13, no. 5, pp. 11–17, 2019.

[35] S. R. Kabir, F. Islam, and A. K. M. Asaduzzaman, "Biogenic silver/silver chloride nanoparticles inhibit human cancer cells proliferation in vitro and Ehrlich ascites carcinoma cells growth in vivo," *Scientific Reports*, vol. 12, Article ID 8909, 2022.

[36] M. El-Far, N. Salah, A. Essam, A. O. Abd El-Azim, and I. M. El-Sherbiny, "Silymarin nanoformulation as potential anticancer agent in experimental Ehrlich ascites carcinoma-bearing animals," *Nanomedicine*, vol. 13, no. 15, pp. 1865–1858, 2018.

[37] H. A. Abosharaf, M. Salah, T. Diab, M. Tsubaki, and T. M. Mohamed, "Biogenic silver nanoparticles induce apoptosis in Ehrlich ascites carcinoma," *Biomedical Research and Therapy*, vol. 7, no. 11, pp. 4100–4113, 2020.

[38] S. Mishra, A. K. Tamta, M. Sarikhani et al., "Subcutaneous Ehrlich ascites carcinoma mice model for studying cancer-induced cardiomyopathy," *Scientific Reports*, vol. 8, Article ID 5599, 2018.

[39] M. I. Sriram, S. B. M. Kanth, K. Kalishwaralal, and S. Gurunathan, "Antitumor activity of silver nanoparticles in

Dalton's lymphoma ascites tumor model," *International Journal of Nanomedicine*, vol. 5, pp. 753–762, 2010.

[40] G. Turgut, Y. Enli, B. Kaptanoğlu, S. Turgut, and O. Genç, "Changes in the levels of MDA and GSH in mice serum, liver and spleen after aluminum administration," *Eastern Journal of Medicine*, vol. 11, no. 1, pp. 7–12, 2006.

[41] E. I. Abdel-Gawad, A. I. Hassan, and S. A. Awwad, "Efficiency of calcium phosphate composite nanoparticles in targeting Ehrlich carcinoma cells transplanted in mice," *Journal of Advanced Research*, vol. 7, no. 1, pp. 143–154, 2016.

[42] J. Baharara, F. Namvar, T. Ramezani, M. Mousavi, and R. Mohamad, "Silver nanoparticles biosynthesized using *Achillea biebersteinii* flower extract: apoptosis induction in MCF-7 cells via caspase activation and regulation of Bax and Bcl-2 gene expression," *Molecules*, vol. 20, no. 2, pp. 2693–2706, 2015.

[43] K. AbouAitah, H. A. Hassan, A. Swiderska-Sroda et al., "Targeted nano-drug delivery of colchicine against colon cancer cells by means of mesoporous silica nanoparticles," *Cancers*, vol. 12, no. 1, Article ID 144, 2020.

[44] D. Chandra, J.-W. Liu, and D. G. Tang, "Early mitochondrial activation and cytochrome *c* up-regulation during apoptosis* 210," *Journal of Biological Chemistry*, vol. 277, no. 52, pp. 50842–50854, 2002.

[45] Y.-G. Yuan, S. Zhang, J.-Y. Hwang, and I.-K. Kong, "Silver nanoparticles potentiates cytotoxicity and apoptotic potential of camptothecin in human cervical cancer cells," *Oxidative Medicine and Cellular Longevity*, vol. 2018, Article ID 6121328, 21 pages, 2018.

[46] M. M. Bradford, "A rapid and sensitive method for the quantitation of microgram quantities of protein utilizing the principle of protein-dye binding," *Analytical Biochemistry*, vol. 72, no. 1-2, pp. 248–254, 1976.

[47] S. Qureshi, O. A. Al-Shabanah, A. M. Al-Bekairi, M. M. Al-Harbi, N. M. Al-Gharably, and M. Raza, "Studies on the cytotoxic, biochemical and anti-carcinogenic potentials of ninhydrin on Ehrlich ascites carcinoma cell-bearing Swiss albino mice," *Investigational New Drugs*, vol. 18, pp. 221–230, 2000.

[48] C. Ashajyothi and K. R. Chandrakanth, "A pilot toxicology study of biogenic silver nanoparticles: *in vivo* by intraperitoneal and intravenous infusion routes in rats," *Journal of Experimental Nanoscience*, vol. 14, no. 1, pp. 89–106, 2019.

[49] N. E.-A. El-Naggar, M. H. Hussein, and A. A. El-Sawah, "Bio-fabrication of silver nanoparticles by phycocyanin, characterization, *in vitro* anticancer activity against breast cancer cell line and *in vivo* cytotxicity," *Scientific Reports*, vol. 7, no. 1, Article ID 10844, 2017.

[50] S. M. El-Sonbaty, "Fungus-mediated synthesis of silver nanoparticles and evaluation of antitumor activity," *Cancer Nanotechnology*, vol. 4, no. 4, pp. 73–79, 2013.

[51] N. E.-A. El-Naggar, M. H. Hussein, and A. A. El-Sawah, "Phycobiliprotein-mediated synthesis of biogenic silver nanoparticles, characterization, *in vitro* and *in vivo* assessment of anticancer activities," *Scientific Reports*, vol. 8, no. 1, Article ID 8925, 2018.

[52] R. M. Abd Al-Rhman, S. R. Ibraheem, and I. Al-Ogaidi, "The effect of silver nanoparticles on cellular and humoral immunity of mice in vivo and in vitro," *Iraqi Journal of Biotechnology*, vol. 15, no. 2, pp. 21–29, 2016.

[53] R. Priya, S. Ilavenil, B. Kaleeswaran, S. Srigopalram, and S. Ravikumar, "Effect of *Lawsonia inermis* on tumor expression induced by Dalton's lymphoma ascites in Swiss albino mice," *Saudi Journal of Biological Sciences*, vol. 18, no. 4, pp. 353–359, 2011.

[54] C. Ashajyothi, H. K. Handral, and K. R. Chandrakanth, "A comparative in vivo scrutiny of biosynthesized copper and zinc oxide nanoparticles by intraperitoneal and intravenous administration routes in rats," *Nanoscale Research Letters*, vol. 13, no. 1, Article ID 93, 2018.

[55] D. Medhat, J. Hussein, M. E. El-Naggar et al., "Effect of Au-dextran NPs as anti-tumor agent against EAC and solid tumor in mice by biochemical evaluations and histopathological investigations," *Biomedicine & Pharmacotherapy*, vol. 91, pp. 1006–1016, 2017.

[56] F. Z. Mohammed, M. Hammad, and M. Al-Dulaimi, "Synthesis of nano sulfur particles and their antitumor activity," *Biochemistry Letters*, vol. 14, no. 1, pp. 109–128, 2018.

[57] M. L. Circu and T. Y. Aw, "Reactive oxygen species, cellular redox systems, and apoptosis," *Free Radical Biology and Medicine*, vol. 48, no. 6, pp. 749–762, 2010.

[58] P. T. Schumacker, "Reactive oxygen species in cancer: a dance with the devil," *Cancer Cell*, vol. 27, no. 2, pp. 156-157, 2015.

[59] A. Bhattacharjee, A. Basu, J. Biswas, T. Sen, and S. Bhattacharya, "Chemoprotective and chemosensitizing properties of selenium nanoparticle (Nano-Se) during adjuvant therapy with cyclophosphamide in tumor-bearing mice," *Molecular and Cellular Biochemistry*, vol. 424, no. 1, pp. 13–33, 2017.

[60] M. Tunçsoy, S. Duran, Ö. Ay, B. Cicik, and C. Erdem, "Effects of copper oxide nanoparticles on antioxidant enzyme activities and on tissue accumulation of *Oreochromis niloticus*," *Bulletin of Environmental Contamination and Toxicology*, vol. 99, pp. 360–364, 2017.

[61] Y.-G. Yuan, Q.-L. Peng, and S. Gurunathan, "Silver nanoparticles enhance the apoptotic potential of gemcitabine in human ovarian cancer cells: combination therapy for effective cancer treatment," *International Journal of Nanomedicine*, vol. 12, pp. 6487–6502, 2017.

[62] T. Bhowmik, P. P. Saha, A. K. DasGupta, and A. Gomes, "Influence of gold nanoparticle tagged snake venom protein toxin NKCT1 on Ehrlich ascites carcinoma (EAC) and EAC induced solid tumor bearing male albino mice," *Current Drug Delivery*, vol. 11, no. 5, pp. 652–664, 2014.

[63] S. J. Jang, I. J. Yang, C. O. Tettey, K. M. Kim, and H. M. Shin, "In-vitro anticancer activity of green synthesized silver nanoparticles on MCF-7 human breast cancer cells," *Materials Science and Engineering: C*, vol. 68, pp. 430–435, 2016.

[64] J. R. Nakkala, R. Mata, and S. R. Sadras, "Green synthesized nano silver: synthesis, physicochemical profiling, antibacterial, anticancer activities and biological in vivo toxicity," *Journal of Colloid and Interface Science*, vol. 499, pp. 33–45, 2017.